

Supporting Information

Electrospun Janus-like Pellicle Displays Coinstantaneous Tri-function of Aeolotropic Conduction, Magnetism and Luminescence

Yunrui Xie, Qianli Ma, Haina Qi, Yan Song, Jiao Tian, Makiyyu Abdullahi Musa, Wensheng Yu,

Xiangting Dong*, Dan Li, Guixia Liu

Key Laboratory of Applied Chemistry and Nanotechnology at Universities of Jilin Province,
Changchun University of Science and Technology, Changchun 130022

*Corresponding author: Fax: 86 0431 85383815; Tel: 86 0431 85582574; E-mail:

dongxiangting888@163.com

Experimental Sections

Chemicals:

Eu₂O₃ (99.99 %), Tb₄O₇ (99.99 %), concentrated nitric acid, benzoic acid (BA), 1,10-phenanthroline (phen), anhydrous ethanol, benzoylperoxide (BPO), aniline (ANI), (1S)-(+)-camphor-10 sulfonic acid (CSA), ammonium persulfate (APS), FeSO₄·7H₂O, FeCl₃·6H₂O, NH₄NO₃, polyethylene glycol (PEG, Mr≈20 000), ammonia, oleic acid (OA), methylmethacrylate (MMA), *N,N*-dimethylformamide (DMF), CHCl₃. Deionized water was homemade. All the chemicals were analytically pure reagents and directly used as received without further purification.

Characterization

The morphologies and structures of the samples were tested *via* a field emission scanning electron microscope (FESEM, XL-30) equipped with an energy-dispersive X-ray spectroscopy

(EDS). An optical microscope (OM, CVM500E) was employed to obtain the images of the samples. The conductive determinations were conducted on a Hall Effect measurement system (ECOPIA HMS-3000). The luminescence of the specimens was analyzed by using a Hitachi fluorescent spectrophotometer F-7000. The crystallographic information was gained by X-ray diffractometer (XRD, Bruker D8 FOCUS) by using a Cu K α radiation source. The magnetism of the samples was detected by a vibrating sample magnetometer (VSE, MPMS SQUID XL). All tests were carried out at room temperature.

Morphology and structure

Fig. S1a is the SEM image of CLJN, where [PANI/PMMA]//[Eu(BA)₃phen/PMMA] Janus-like microribbons are disordered and the surface of microribbons is smooth. The width and thickness of [PANI/PMMA]//[Eu(BA)₃phen/PMMA] Janus-like microribbons in CLJN respectively are *ca.* 21.43 \pm 0.72 μ m (**Fig. S2a**) and 1.3 μ m. **Fig. S1b** and **Fig. S1c** respectively are SEM images of CLCA and CLCN. PANI/PMMA/Eu(BA)₃phen composite microribbons are aligned in the same direction and the width and thickness respectively are *ca.* 19.33 \pm 0.41 μ m (**Fig. S2b**) and 1.3 μ m. In CLCN, PANI/PMMA/Eu(BA)₃phen composite microribbons are disordered, and the width and thickness of respectively are *ca.* 19.07 \pm 0.41 μ m (**Fig. S2c**) and 1.3 μ m. In MLJN (**Fig. S1d**), [Fe₃O₄/PMMA]//[Tb(BA)₃phen/PMMA] Janus-like microribbons are disordered and the surface of microribbons is slightly rough. The width and thickness of [Fe₃O₄/PMMA]//[Tb(BA)₃phen/PMMA] Janus-like microribbons in MLJN respectively are *ca.* 19.30 \pm 0.85 μ m (**Fig. S2d**) and 1.3 μ m. **Fig. S1e** and **Fig. S1f** respectively are SEM images of MLCA and MLCN. It can be seen that almost Fe₃O₄/PMMA/Tb(BA)₃phen/PMMA composite microribbons in MLCA are aligned in the same direction and the width and thickness respectively are *ca.* 20.54 \pm 0.23 μ m (**Fig. S2e**) and 1.3 μ m. In MLCN, the surface of disordered Fe₃O₄/PMMA/Tb(BA)₃phen/PMMA composite

microribbons is slightly rough, and the width and thickness of respectively are *ca.* 18.32 ± 0.25 μm (**Fig. S2f**) and 1.3 μm .

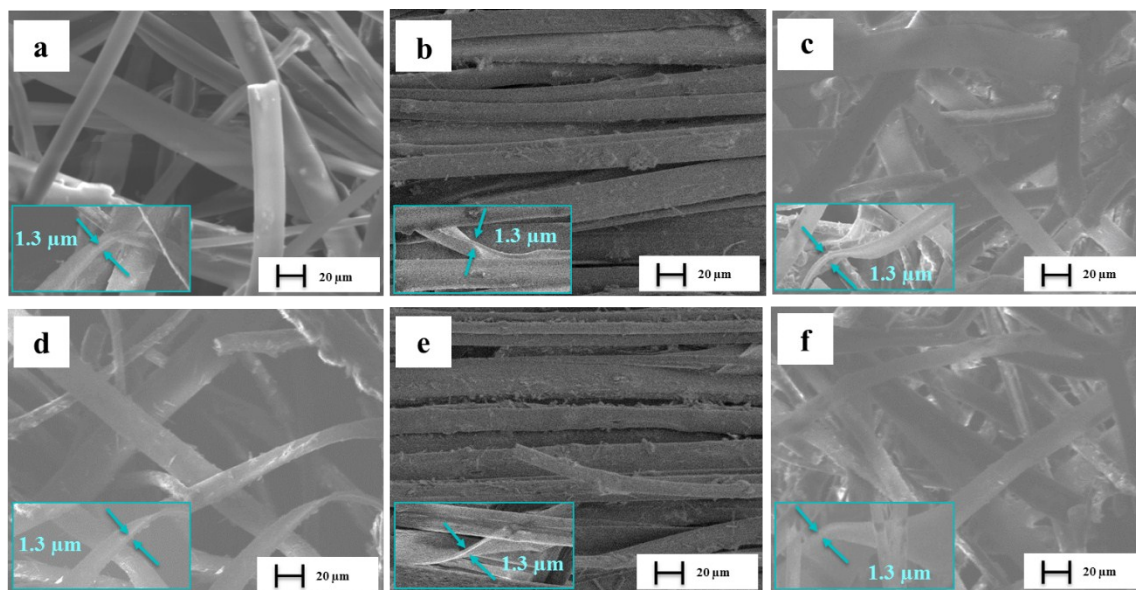


Fig. S1 SEM images of CLJN (a), CLCA (b), CLCN (c), MLJN (d), MLCA (e) and MLCN

(f)

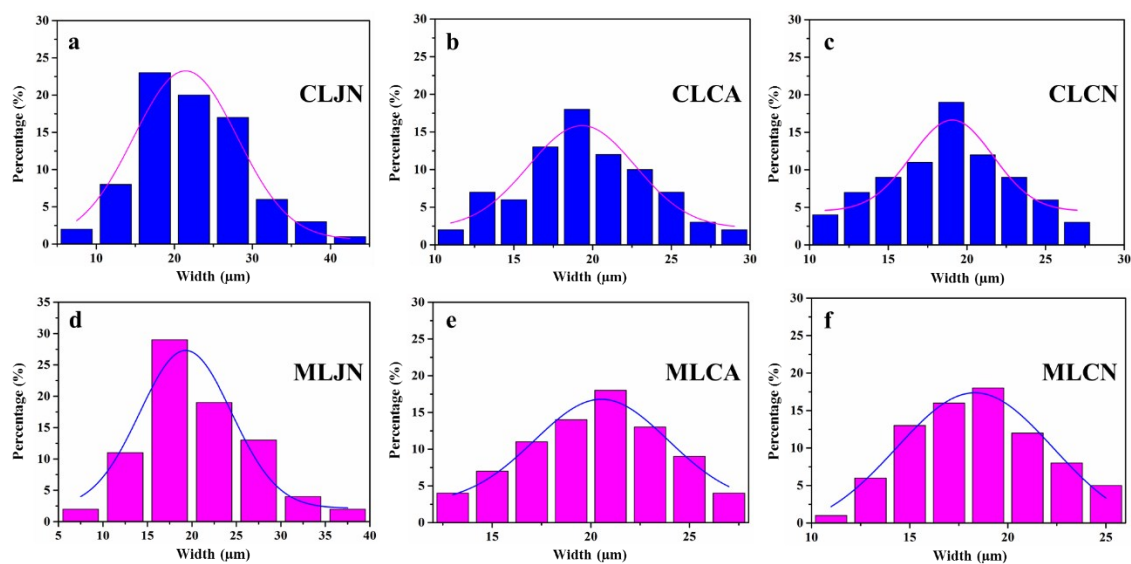


Fig. S2 Width distribution histograms of CLJN (a), CLCA (b), CLCN (c), MLJN (d), MLCA

(e) and MLCN (f)

A clear interface is observed between approximately transparent $\text{Eu}(\text{BA})_3\text{phen}/\text{PMMA}$ and the dark green PANI/PMMA , as shown in **Fig. S3a**. It proves that $[\text{PANI}/\text{PMMA}]/[\text{Eu}(\text{BA})_3\text{phen}/\text{PMMA}]$ Janus-like microribbon has favorable Janus-like structure in CLJN. However, no a clear interface in $\text{PANI}/\text{PMMA}/\text{Eu}(\text{BA})_3\text{phen}$ composite microribbons for CLCA (**Fig. S3b**) and CLCN (**Fig. S3c**) is observed. As seen from **Fig. S3d**, a clear interface is observed between approximately transparent $\text{Tb}(\text{BA})_3\text{phen}/\text{PMMA}$ and brown $\text{Fe}_3\text{O}_4/\text{PMMA}$, which indicates that $[\text{Fe}_3\text{O}_4/\text{PMMA}]/[\text{Tb}(\text{BA})_3\text{phen}/\text{PMMA}]$ Janus-like microribbon is successfully prepared in MLJN. For MLCA (**Fig. S3e**) and MLCN (**Fig. S3f**), no apparent interface is found in $\text{Fe}_3\text{O}_4/\text{PMMA}/\text{Tb}(\text{BA})_3\text{phen}/\text{PMMA}$ composite microribbons. These results show that Janus-like microribbon can achieve micro-zoning and reduce interferences among different functional substances. However, composite microribbon cannot achieve micro-zoning and cause harmful influences among different properties.

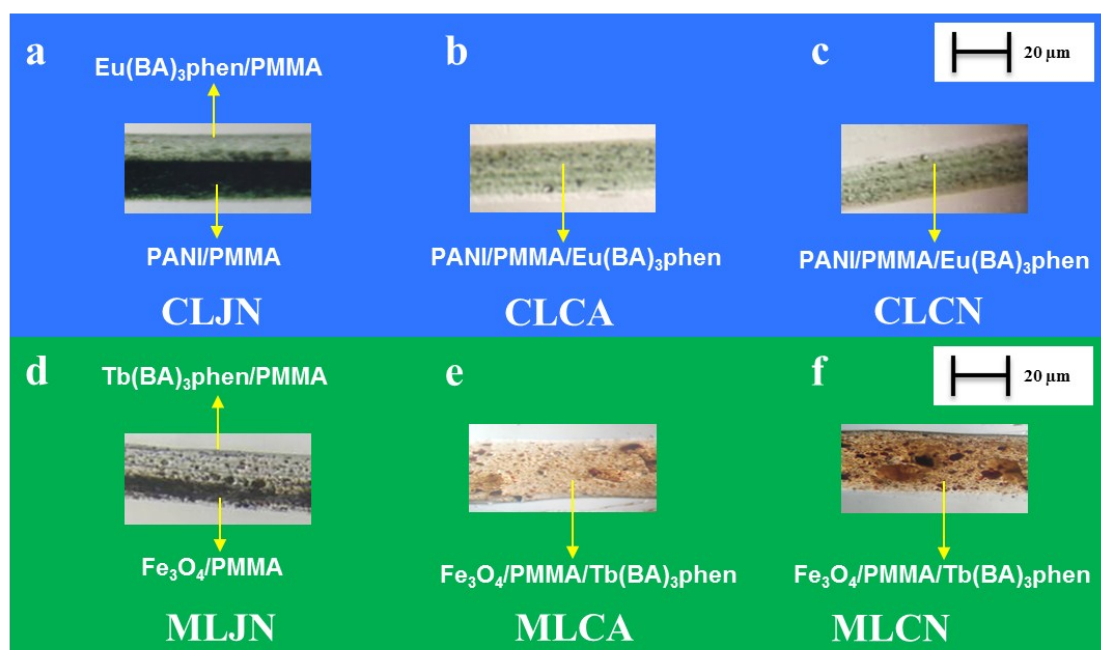


Fig. S3 OM images of single $[\text{PANI}/\text{PMMA}]/[\text{Eu}(\text{BA})_3\text{phen}/\text{PMMA}]$ Janus-like microribbon in CLJN (a), single $\text{PANI}/\text{PMMA}/\text{Eu}(\text{BA})_3\text{phen}$ composite microribbon in CLCA (b), single $\text{PANI}/\text{PMMA}/\text{Eu}(\text{BA})_3\text{phen}$ composite microribbon in CLCN (c), single

[Fe₃O₄/PMMA]/[Tb(BA)₃phen/PMMA] Janus-like microribbon in MLJN (d), single Fe₃O₄/PMMA/Tb(BA)₃phen/PMMA composite microribbons in MLCA (e) and single Fe₃O₄/PMMA/Tb(BA)₃phen/PMMA composite microribbon in MLCN (f)

Crystallography

Fig. S4 demonstrates the XRD patterns of ML layer, MLJN, MLCA and MLCN doped with the same amounts of Fe₃O₄ NPs (Fe₃O₄:PMMA=1:1). The diffraction peaks of MLJN, MLCA and MLCN can well match the standard card (PDF # 75-0449) of cubic phase of Fe₃O₄ and ML layer. No diffraction peaks of impurities are detected, indicating that pure-phase Fe₃O₄ NPs are successfully introduced into ML layer and three contrast samples.

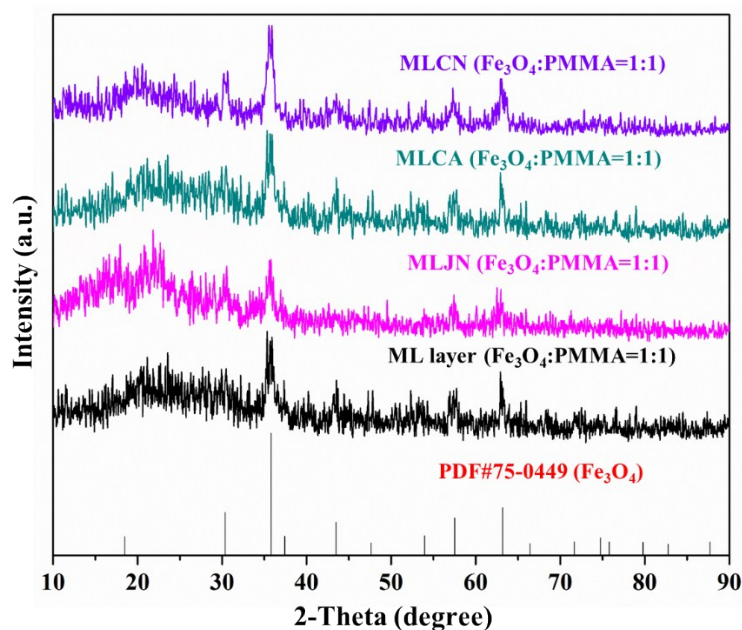


Fig. S4 XRD patterns of ML layer, MLJN, MLCA and MLCN doped with the same amounts of Fe₃O₄ NPs (Fe₃O₄:PMMA=1:1)